DALTON

Molecular mechanics calculations on imine and mixed-ligand systems of Co^{III}, Ni^{II} and Cu^{II}†

Robert J. Deeth* and Veronica J. Paget

Inorganic Computational Chemistry Group, Department of Chemistry, University of Warwick, Coventry CV4 7AL, UK

The force field for the cellular ligand field stabilisation energy/molecular mechanics (CLFSE/MM) method has been applied to 28 transition-metal complexes. Computed and experimental structures are compared for 12 ML_xCl_{6-x} species (M = Co^{III} or Ni^{II}; L = amine donor; x = 6 or 4), 12 MA_xB_{6-x} compounds (M = Ni^{II} or Cu^{II}; A = imine, B = amine; x = 6, 4 or 3), one five-co-ordinate copper(II) imine–amine complex and three four-co-ordinate copper(II) imine and imine–amine molecules. For π-bonding ligands a stronger donor interaction is associated with a larger positive value of the CLF e_π parameter but, due to the use of a crystal field type barycentre, the CLFSE actually goes up. The CLFSE thus has the wrong form for treating the π contributions to bond stretching and distance-dependent e_π parameters are inappropriate. However, the desired bond lengths can be obtained by modifying the Morse function and e_σ terms. The π contribution to the L–M–L angle bending operates in the correct sense but is small and can also be accommodated by altering the magnitude of e_σ. For asymmetric π interactions ($e_{\pi x} \neq e_{\pi y}$) there is no effect on the M–L torsional potential for low-spin d^6, high-spin d^8 and d^9 configurations where the π-symmetry d orbitals are completely filled. Hence, only the σ-bonding contributions to the CLFSE are retained. This approach still gives good agreement with experimental structures, even for formally π-bonding ligands, with average root-mean-square errors in M–L lengths and L–M–L angles of about 0.02 Å and 3° for Co^{III}, Ni^{II} and four co-ordinate Cu^{II}, excluding $[Cu(bipy)_2]^{2+}$ (bipy = 2,2′-bipyridyl), and about 0.05 Å and 4° respectively for six-co-ordinate Cu^{II}, excluding $[Cu(terpy)_2]^{2+}$ (terpy = 2,2′:6′,2″-terpyridyl). The subtle interplay between the axial Ni–Cl and equatorial Ni–N distances in *trans*-$[NiN_4Cl_2]$ macrocyclic species is reproduced for the first time by an MM-based approach. However, the model appears to give relatively poor agreement for $[Cu(bipy)_2(NH_3)]^{2+}$, $[Cu(terpy)_2]^{2+}$ and $[Cu(bipy)_2]^{2+}$. For the five-co-ordinate complex this is due to the intrinsic plasticity of five-co-ordinate copper(II) species. The energy difference between the limiting trigonal-bipyramidal and square-pyramidal geometries is only a few kcal mol^{-1}. For $[Cu(terpy)_2]^{2+}$ the limiting geometries of tetragonally elongated and compressed octahedra are also within a few kcal mol^{-1} although the present set of parameters overestimates the ligand contribution and predicts a compressed geometry. The calculated structure of $[Cu(bipy)_2]^{2+}$ is too flat but for four-co-ordinate species it is shown, using $[CuCl_4]^{2-}$ as an example, that there are several ways to induce a tetrahedral distortion. The most satisfactory method is to include charges on Cu and the ligand donors whereupon the geometries of $[CuCl_4]^{2-}$ and $[Cu(bipy)_2]^{2+}$ distort to the required flattened tetrahedral structures.

Molecular mechanics (MM) is well established in co-ordination chemistry and has been used to determine structures, isomer and conformer ratios, and metal-ion selectivities for a range of metals and ligands.[2–11] Our contributions have so far focused on special problems, such as Jahn–Teller active copper(II) complexes[12] which cause difficulties for conventional MM schemes, and on developing transferable force fields which can model both high- and low-spin nickel(II) species simultaneously.[1] This latter feature requires two separate force fields for conventional MM therefore limiting the possibilities for modelling spin-cross-over behaviour. Our approach is to extend the conventional MM scheme with a cellular ligand field stabilisation energy (CLFSE) term which explicitly treats the electronic effects arising from changes in the d-orbital energies.

To date, we have only considered amine complexes since σ-bonding-only ligands are the simplest to treat within the CLF formalism.[13,14] Here we report on the extension of the CLFSE/MM method to transition-metal complexes of Cu^{II}, Ni^{II} and Co^{III} with various combinations of σ-bonding amine plus potentially π-bonding imine and chloride ligands.

† Molecular Mechanics for Co-ordination Complexes. Part 2.[1] *Supplementary data available* (No. SUP 57196, 6 pp.): force-field parameters and functional forms. See Instructions for Authors, *J. Chem. Soc., Dalton Trans.*, 1997, Issue 1.
Non-SI unit employed: cal = 4.184 J.

Theoretical

A full account of the CLFSE/MM implementation has been published[1] so only a brief outline is given here. The general form for the total strain energy, E_{tot}, is given in equation (1),

$$E_{tot} = E_{str} + E_{bend} + E_{tor} + E_{vdw} + \text{CLFSE} \qquad (1)$$

where the terms refer respectively to the bond stretching, angle bending, torsional, non-bonding and CLFSE interactions. The first four terms are treated *via* conventional MM expressions with the following provisos: E_{str} is described by a Morse function, there are no E_{bend} or E_{tor} terms involving the metal centre and E_{vdw} includes explicit ligand–ligand 1,3 interactions. Electrostatic interactions are not included although this matter is discussed further below.

The CLFSE for a d^n system is given by equation (2), where

$$\text{CLFSE} = \sum_{i=1}^{n} \rho(d_i)\varepsilon(d_i) \qquad (2)$$

$\rho(d_i)$ is the d-orbital occupation number and $\varepsilon(d_i)$ the energy of orbital d_i. The d-orbital energies are expressed in terms of the cellular ligand field (CLF) parameters e_λ (where $\lambda = \sigma$, π_x or π_y)[13,14] which are in turn expressed as a function of the M–L distance, r. For simple σ-bonding-only ligands like amines ($e_{\pi x} = e_{\pi y} = 0$) a linear dependence of e_σ *vs.* r was chosen

[equation (3)] where, a_0 and a_1 are empirically derived constants

$$e_\sigma = a_0 + a_1 r \quad (3)$$

and the resulting values for e_σ are not required, for example, to reproduce the d–d spectrum although this will be roughly true. Similar expressions can be used for $e_{\pi x}$ and $e_{\pi y}$ with the condition that a_0 and a_1 are chosen so as to retain the same sign for e_π over the anticipated range of M–L distances. This contrasts with e_σ which is permitted to become negative at long bond lengths.

Modelling π-bonding ligands

One of our perceived advantages of using the CLF model within a MM framework was the ability to separate the M–L bonding into its individual σ and π components. However, for donor ligands where e_π is positive it turns out that π interactions work in the wrong sense.

The CLFSE needs to reflect the overall electronic contributions to the M–L bonding in a complex. The energy changes of the essentially antibonding d orbitals are used implicitly to monitor the energy changes of the associated bonding functions. Considering the CLFSE alone, we required that shortening and strengthening a given M–L bond, which will lower the total electronic energy, should also be energetically favoured in that the CLFSE becomes increasingly negative. Such is the case for σ bonding. Considering an octahedral species for illustrative purposes, as the bond strengthens e_σ becomes more positive and Δ_{oct} becomes larger. Since the CLFSE is proportional to the negative of Δ_{oct}, the CLFSE becomes more negative as required. However, since the π-symmetry d orbitals are lower in energy than the global barycentre, increasing e_π pushes the d_π orbitals up in energy which tends to reduce the magnitude of the CLFSE implying an overall destabilisation. Of course, any rise in the d_π orbitals is countered by a fall in the corresponding bonding functions such that overall there will still be a net electronic stabilisation if the d_π orbitals have one or more vacancies or no net energy change if they are completely filled. However, these bonding orbitals are not considered explicitly and thus, as a function of M–L distance, the π-donor contribution to the CLFSE gives the opposite behaviour to that desired. This is due to the use of a crystal field barycentre for the d orbitals which arises from expanding the ligand-field potential in terms of spherical harmonics as described by Gerloch.[13] Presumably, π interactions could be modelled correctly if we described the d-orbital energies relative to the CLF barycentre. However, the present approach gives good molecular structures (see below) and, for the present, we remove any bond-length dependence for e_π by setting the value of a_1 in equation (3) to zero for π-donor ligands.

Nevertheless, fixed e_π values can still contribute to L–M–L angle bending as well as to the torsional potential for rotations about the M–L bond providing, in the latter case, that the π interaction is asymmetric. However, the lack of any distance dependence gives the d_π functions their own barycentre such that, if these orbitals each contain the same number of electrons, rotation about the M–L bond cannot affect the overall CLFSE. This is the case for low-spin d^6 Co^{III}, high-spin d^8 Ni^{II} and d^9 Cu^{II}. Hence, a σ-bonding-only model is sufficient for the bond stretch and torsional components of the CLFSE for these configurations even though the ligands have a π-bonding capability. The same will not be true for complexes where the d_π functions are not symmetrically filled as in, for example, any octahedral system which formally has an orbital-triplet ground state. We are currently investigating whether the magnitude of any π effects on torsion angles is large enough to influence calculated structures significantly.

Finally, e_π can, in principle, play a role in determining L–M–L angles. However, it turns out that for any reasonable values of this parameter the effect is fairly small and can be accommodated by reducing the magnitude of e_σ. The particular case of the balance between tetrahedral and planar co-ordination is considered in detail below.

Computational Details

The in-house molecular mechanics program DOMMINO* was used to compute the structures of the 28 compounds displayed schematically in Fig. 1 and listed in Table 1. The latter also gives the ligand abbreviations and their full names. Initial structures used for minimisation were obtained from the Cambridge Structural Database (CSD).[15] A full listing of the force-field parameters has been deposited as SUP 57196.

Results and Discussion

The complexes shown in Fig. 1 have been divided into several related sets which are discussed in turn below. Where relevant, 'organic' connections between donor atoms or groups are restricted to saturated alkane chains.

Cobalt(III) amine complexes 1–4

Low-spin d^6 cobalt(III) complexes have a well defined octahedral stereochemistry which is relatively straightforward to treat within a conventional MM scheme.[1,42] The CLFSE/MM parameters were developed for $Co–N_{amine}$ first to show that we can easily mimic the results from conventional force fields and secondly for use with the mixed amine–chloro complexes described later.

The observed and calculated Co–N bond lengths and N–Co–N angles are given in Table 2 and, where possible, compared with the results from the treatment of Hancock.[42] The r.m.s. errors for these data and for the M–N–C and 'organic' part of the molecule (excluding any features involving hydrogen) have been deposited as SUP 57196. Overall, the performance of the CLFSE/MM method with respect to the metal co-ordination environment is at least as good as that of conventional MM. The average r.m.s. errors in metal–ligand bond lengths and angles are only 0.018 Å and 2.3° respectively.

Mixed chloro–amine complexes $[MN_4Cl_2]$ 5–12 (M = Ni^{II} or Co^{III})

The usefulness of the CLFSE/MM method depends on its ability to treat mixed-ligand systems. As a first step, parameters for monatomic chloride have been developed and merged with the existing metal–amine force field. The average observed and calculated M–L bond lengths and angles for the $[MN_4Cl_2]$ complexes shown in Fig. 1 are given in Table 3. An indication of the performance for the rest of the molecule is given in SUP 57196, where r.m.s. errors for the M–N–C angles and the remaining 'organic' bond lengths and angles are presented. The calculated structures are in good agreement with experimental geometries. The overall M–L and L–M–L r.m.s. errors for all eight complexes are 0.025 Å and 1.4° respectively with the worst case being for $[Ni(cyclam)Cl_2]$ **9** where the Ni–N bond lengths are computed to be 0.05 Å too short.

An interesting feature of these complexes is the interplay between the M–Cl and M–N bonds. For the cobalt(III) species there is not much variation (either calculated or observed) in the Co–Cl and Co–N distances but for the nickel(II) species the observed Ni–Cl bonds vary by up to 0.09 Å. The computed Ni–Cl lengths correlate well with experiment both for the *trans* species, where both Ni–Cl bonds are essentially the same, and

* Based on molecular mechanics software kindly supplied by Dr. D. J. Osguthorpe, Molecular Graphics Unit, University of Bath and modified to include the CLFSE contribution.

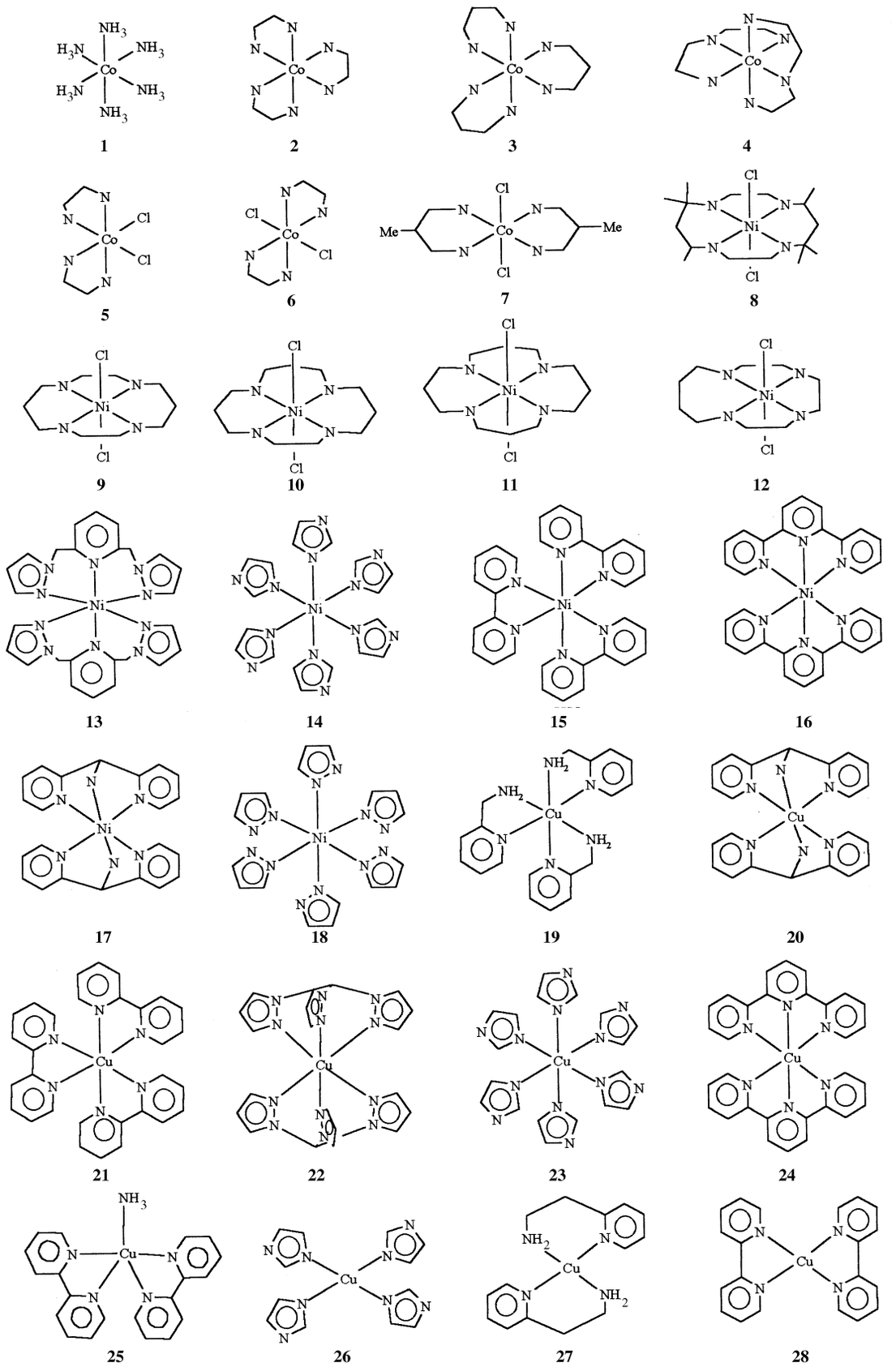

Fig. 1 Schematic diagrams of the complexes used in this study. See Table 1 for details

for $[NiL^3Cl_2]$ **11** where they differ by 0.09 Å. The latter feature is due to the configuration of the skeletal structure.[30] Two of the carbon atoms are disposed close to one of the axial coordination sites, causing steric hindrance which results in the lengthening of one axial bond. Overall, the CLFSE/MM scheme gives a good description of the reported synergism[43] between the axial monodentate ligand and the in-plane macrocyclic ligand. However, it should be noted that the bond length

Table 1 Chemical formulae, full ligand names and Cambridge Structural Database (CSD) reference codes[15] for the molecules shown in Fig. 1

	Complex	Ligand name	CSD refcode	Ref.
1	$[Co(NH_3)_6]^{2+}$		EDTACO	16
2	$[Co(en)_3]^{2+}$	Ethane-1,2-diamine	ENCOPN	17
3	$[Co(tn)_3]^{2+}$	1,3-Diaminopropane	COTNCL	18
4	$[Co(bapa)_2]^{2+}$	Bis(3-aminopropyl)amine	BOKYEF	19
5	*cis*-$[Co(en)_2Cl_2]$		CENCOC	20
6	*trans*-$[Co(en)_2CL_2]$		CENCOS	21
7	$[Co(metn)_2Cl_2]$	2-Methylpropane-1,3-diamine	CAWPOF	22
8	$[NiL^1Cl_2]$	*meso*-7*R*(*S*),14*S*(*R*)-5,5,7,12,12,14-Hexamethyl-1,4,8,11-tetraazacyclotetradecane	MAZNIB	23
9	$[Ni(cyclam)Cl_2]$	1,4,8,11-Tetraazacyclotetradecane	TAZDNC01	24
10	$[NiL^2Cl_2]$	1,4,8,12-Tetraazacyclopentadecane	DITVEH*	24
11	$[NiL^3Cl_2]$	1,5,9,13-Tetraazacyclohexadecane	DITVIL	24
12	$[NiL^4Cl_2]$	1,4,7,10-Tetraazacyclotetradecane	BOZZIZ	25
13	$[Ni(bpzpy)_2]^{2+}$	2,6-Bis(pyrazol-1-ylmethyl)pyridine	FILYOO	26
14	$[Ni(Him)_6]^{2+}$	Imidazole	HIMZNI	27
15	$[Ni(bipy)_3]^{2+}$	2,2′-Bipyridyl	BPYNIS	28
16	$[Ni(terpy)_2]^{2+}$	2,2′: 6′,2″-Terpyridyl	BIKJUA	29
17	$[Ni(dpma)_2]^{2+}$	Di-2-pyridylmethanamine	JUNCOK	30
18	$[Ni(Hpz)_2]^{2+}$	Pyrazole	PYZNIN	31
19	$[Cu(amp)_3]^{2+}$	2-(Aminomethyl)pyridine	SITBUS	32
20	$[Cu(dpma)_2]^{2+}$		JUNDAX	33
21	$[Cu(bipy)_3]^{2+}$		TBPYCU	34
22	$[Cu(tpzm)_2]^{2+}$	Tris(pyrazol-1-yl)methane	SUHCAZ	35
23	$[Cu(Him)_6]^{2+}$		IMZCUN	36
24	$[Cu(terpy)_2]^{2+}$		SIBWEF	37
25	$[Cu(bipy)_2(NH_3)]^{2+}$		ABPYCU	38
26	$[Cu(Him)_4]^{2+}$		TIMZCU	39
27	$[Cu(aep)_2]^{2+}$	2-(2-Aminoethyl)pyridine	CUAEPP10	40
28	$[Cu(bipy)_2]^{2+}$		BPYCUP	41

* Data taken directly from ref. 24.

Table 2 Observed and calculated bond lengths (Å) and angles (°) for six-co-ordinate cobalt(III) amine complexes (see Fig. 1 for structural diagrams). Where appropriate, comparisons with the work of Hancock[42] are made

	$[Co(NH_3)_6]^{2+}$			$[Co(en)_3]^{2+}$		
	calc.	obs.[16]	Hancock	calc.	obs.[17]	Hancock
Co–N	1.96	1.96	1.96	1.96	1.96	1.96
N–Co–N (average)	90.0 179.8	90.0 179.7	90	90.0 176.0	90.6 175.6	88.0
	$[Co(tn)_3]^{2+}$			$[Co(bapa)_2]^{2+}$		
	calc.	obs.[18]	Hancock	calc.	obs.[19]	Hancock
Co–N	1.99	1.98	1.99	1.99 2.02	2.00 2.04	1.97 2.04
N–Co–N (average)	90.0 178.6	90.0 177.8	94.7	90.0 176.9	90.1 174.6	94.5

changes which Ito *et al.*[43] base their arguments on are only of the order of a few hundredths of an Ångstrom which are barely significant. Nevertheless, our d-electron term provides a 'through bond' connection and is the first MM-based approach capable of reproducing such subtle structural effects.

The Ni–Cl parameters do not, however, reproduce the structures of $[NiCl_n]^{2-n}$ ($n = 4$ or 6) and generate bonds which are too long. The computed Ni–Cl distances in complexes **8**–**12** are between 2.48 and 2.56 Å. These values should be compared with the notional 'strain free' Ni–Cl contact of 2.39 Å computed using only the Morse function and the CLFSE. The longer values found for the macrocyclic species reflect the intramolecular interactions between the axial chlorides and the ring systems. Such interactions are absent for $[NiCl_n]^{2-n}$ ($n = 4$ or 6) and bond lengths close to the 'strain free' value result. However, the experimental Ni–Cl distance in, for example, $[NiCl_4]^{2-}$ is 2.26 Å.[44] The present force field requires some further tuning.

Imine and mixed amine–imine complexes of Ni^{II} and Cu^{II} 13–28

Unsaturated nitrogen-donor ligands are extremely important in co-ordination chemistry. For example, metalloproteins often bind transition metals, especially Cu^{II}, *via* the imidazole groups on histidine side chains. The observed and calculated metal–ligand bond lengths and angles are reported for six $Ni^{II}N_6$ complexes (Table 4), six six-co-ordinate copper(II) complexes (Table 5) and one five-co-ordinate copper(II) plus three four-co-ordinate copper(II) complexes (Table 6). As before, the relevant r.m.s. errors for these data and for the remaining 'organic' parts of the molecules have been deposited as SUP 57196.

Table 3 Observed and calculated bond lengths (Å) and angles (°) for six-co-ordinate cobalt(III) and nickel(II) MN_4Cl_2 amine–chloride complexes (see Fig. 1 for structural diagrams)

	cis-$[Co(en)_2Cl_2]$		*trans*-$[Co(en)_2Cl_2]$		$[Co(metn)_2]^{2+}$	
	calc.	obs.[20]	calc.	obs.[21]	calc.	obs.[22]
Co–Cl	2.25	2.26	2.27	2.24	2.25	2.27
Co–N	1.96	1.97	1.95	1.95	1.97	2.00
Cl–Co–Cl	89.5	93.1	180.0	178.3	180.0	—
Cl–Co–N	90.4 177.4	89.5 178.1	90.0 180.0	90.0 178.2		
N–Co–N	89.6 177.1	90.0 178.1	90.0	90.7	88.3 91.7	88.1 89.9
	$[NiL^1Cl_2]$		$[Ni(cyclam)Cl_2]$			
	calc.	obs.[23]	calc.	obs.[24]		
Ni–Cl	2.56	2.56	2.50	2.51		
Ni–N	2.06 2.02	2.10 2.06	2.02	2.07		
N–Ni–Cl	90.0	90.0	90.0	90.0		
N–Ni–N	90.0 180.0	90.0 180.0	90.0 180.0	90.0 180.0		
Cl–Ni–Cl	179.9	180.0	180.0	180.0		
	$[NiL^2Cl_2]$		$[NiL^3Cl_2]$		$[NiL^4Cl_2]$	
	calc.	obs.[24]	calc.	obs.[24]	calc.	obs.[25]
Ni–Cl	2.50	2.50	2.52 2.44	2.54 2.43	2.53	2.55
Ni–N	2.07 2.13	2.10 2.12	2.28 2.16 2.13 2.13	2.21 2.19 2.14 2.14	2.02 2.04	2.06 2.08
N–Ni–Cl	90.0		90.0	90.1	90.1	90.1
N–Ni–N	90.1 173.7		89.9 173.2	90.0 172.8	90.7 163.1	90.7 161.7
Cl–Ni–Cl	176.1		174.3	172.9	177.3	177.6

The data for the nickel(II) complexes (Table 4) are all in excellent agreement with the observed structures, the worst cases being for $[Ni(terpy)_2]^{2+}$ **16** where a Ni–N bond length is calculated 0.03 Å too short and for $[Ni(bipy)_3]^{2+}$ **15** where the *trans* N–Ni–N angle is calculated some 5° too large. However, the average r.m.s. errors for complexes **13**–**25** are only 0.011 Å and 2.4° for Ni–N distances and N–Ni–N angles respectively.

As found previously,[12] the CLFSE/MM model automatically generates tetragonal distortions for six-co-ordinate copper(II) complexes (Table 5). Tetragonal elongations are predicted except for $[Cu(terpy)_2]^{2+}$ **24** which is computed to have a compressed geometry. The room-temperature crystallographic study of the $[PF_6]^-$ salt also yields a compressed structure[37] (see Table 5) while the nitrate salt has an elongated copper centre.[45] However, variable-temperature electron spin resonance measurements indicate that the former is a result of a dynamic Jahn–Teller effect and that the true low-temperature co-ordination geometry is tetragonally elongated.[37] The experimental energy difference between elongated and compressed structures is evidently small. If the Cu–N distances are constrained to those found for $[Cu(terpy)_2][NO_3]_2$[45] (*viz.* 1.97, 2.02, 2.09, 2.09, 2.29 and 2.29 Å) while the rest of the molecule is relaxed, the energy of the elongated system is computed to be less than 3 kcal mol^{-1} higher than for the compressed complex. The nickel(II) analogue shows a definite tetragonal compression presumably imposed by the terpy ligand and although the CLFSE alone favours an elongated structure it is not sufficient to overcome the ligand's tendency to compress the structure. However, the difference is of the order of crystal-packing energies.

For the remaining CuN_6 species the magnitudes of the elongations are reproduced quite well. Given the 'plasticity' of copper(II) complexes, the geometries of these species are also susceptible to crystal-packing forces while the force field represents some averaged environment. To first order, the Q_0 mode of the $E\otimes\varepsilon$ vibronic coupling problem yields an axial bond length change of $-2\delta x$ if the equatorial distance changes by δx.[46] Relative to experiment, therefore, we expect (and find) that if the $Cu–N_{eq}$ distance is computed to be smaller than observed the $Cu–N_{ax}$ contact is longer than experiment. This pattern is found for $[Cu(Him)_6]^{2+}$ **23**, $[Cu(dpma)_2]^{2+}$ **20** and $[Cu(tpzm)_2]^{2+}$

Table 4 Observed and calculated bond lengths (Å) and angles (°) for six-co-ordinate nickel(II) imine complexes (see Fig. 1 for structural diagrams)

	$[Ni(bpzpy)_2]^{2+}$		$[Ni(Him)_6]^{2+}$		$[Ni(bipy)_3]^{2+}$	
	calc.	obs.[26]	calc.	obs.[27]	calc.	obs.[28]
$Ni–N_{py}$	2.15	2.16			2.08	2.09
$Ni–N_{pz}$	2.07	2.08	2.10	2.13		
N–Ni–N	90.0	90.0	90.0	90.2	90.0	90.2
(average)	177.2	177.7	180.0	180.0	175.4	169.7

	$[Ni(terpy)_2]^{2+}$		$[Ni(dpma)_2]^{2+}$		$[Ni(Hpz)_6]^{2+}$	
	calc.	obs.[29]	calc.	obs.[30]	calc.	obs.[31]
$Ni–N_{py}$	2.14	2.13	2.10	2.11		
	1.99	2.02				
$Ni–N_{am}$			2.12	2.11		
$Ni–N_{pz}$					2.11	2.13
N–Ni–N	90.6	90.4	90.0	90.0	90.0	90.0
(average)	166.7	163.2	180.0	180.0	180.0	180.0

22. The observed and calculated elongations are about the same for $[Cu(amp)_3]^{2+}$ **19**. For $[Cu(bipy)_3]^{2+}$ **21** the two observed $Cu–N_{ax}$ distances are different, presumably due to an asymmetric crystal environment, while theory gives identical bond lengths. However, the average observed $Cu–N_{ax}$ contact is only 0.02 Å shorter than the calculated value.

The orientation of the planes of these unsaturated ligands is also expected to be affected by crystal packing. For example, the observed $[Cu(Him)_6]^{2+}$ structure shows tilting of the axial ligand about the Cu–N bond in order that the H of the ligand may take part in hydrogen bonding with the O of the $[NO_3]^-$ counter ion.[36] This tilting was not reproduced by the molecular mechanics calculation as interactions of the complex with counter ions, and other crystal-packing forces, have yet to be included.

For the five-co-ordinate case (Table 6) the calculated structure displays square-based pyramidal geometry whereas the observed structure is approximately trigonal bipyramidal. The counter ion for the experimental structure is $[BF_4]^-$, and there is apparently hydrogen bonding between the F of the $[BF_4]^-$ and the H on the ammonia.[38] Experimentally, five-co-ordinate copper(II) complexes frequently display intermediate and variable structures from near trigonal bipyramidal to near square pyramidal with quite dramatic effects on the Cu–L distances. This is shown, for example, by complexes of the type $[Cu(bipy)_2X]^{n+}$.[47,48] Our previous observations[12] demonstrated that the CLFSE/MM model favours a square-pyramidal symmetry but that the analogous trigonal-bipyramidal complex has a very similar energy. Thus, the apparent discrepancy between theory and experiment is particularly marked for five-co-ordinate copper(II) complexes but it is not energetically significant. If the surrounding lattice were explicitly included in the calculations then better agreement between calculated and observed structures would be expected.

Planar four-co-ordinate d^9 species are usually less plastic than five- and six-co-ordinate complexes since the former are at the limit of tetragonal elongation. Thus, one would expect this class of copper(II) complex to give the best agreement between the calculated and observed structures. This is indeed the case for $[Cu(Him)_4]^{2+}$ **26** and $[Cu(aep)_2]^{2+}$ **27** where the maximum Cu–N deviation from the observed bond length is only 0.03 Å (Table 6). However, for $[Cu(bipy)_2]^{2+}$ **28** poor agreement is found. Experimentally, the complex displays distorted-tetrahedral geometry,[41] whereas the calculated structure is nearer a square plane.

Tetrahedral *versus* planar co-ordination: the role of electrostatics

For d^9 species there is a subtle balance between ligand–ligand repulsion, which favours a tetrahedral structure, and the d-electron stabilisation energy which favours planar co-ordination. Experimentally, $[CuCl_4]^{2-}$ usually has a flattened tetrahedral D_{2d} geometry[49] and various *ab initio* quantum-chemical calculations have confirmed this as the lowest-energy structure in the gas phase.[50] However, the energy difference between tetrahedral and planar co-ordination is small and the latter is observed with a suitable choice of counter cation. The d-electron energies dominate in the present CLFSE/MM force field as illustrated by the modelling of $[CuCl_4]^{2-}$. Assuming D_{2d} symmetry and a Cu–Cl distance of 2.26 Å, the total strain energy can be expressed as a function of θ, the acute angle between the *z* axis and the Cu–Cl vector (see Appendix). For tetrahedral co-ordination $\theta = 54.7°$ while for a planar system, $\theta = 90°$.

Assuming a fixed value of $e_\sigma = 4000\ cm^{-1}$, there are three factors which can induce a tetrahedral geometry: π bonding, non-bonding ligand–ligand repulsion and electrostatic ligand–ligand repulsion. These terms are related respectively to $e_\pi(Cl)$, A_{Cl} from the E_{vdw} expression and the charge on Cl, ρ(Cl). Considering the CLFSE alone, it is instructive to analyse what value e_π must adopt in order to generate a tetrahedral structure. The d^9 CLFSE for T_d and D_{4h} symmetries are given by equations (4) and (5). Equating equation (4) to (5) and setting $R = e_\pi/e_\sigma$ gives

$$d^9\ CLFSE(T_d) = (-24e_\sigma + 32e_\pi)/45 \qquad (4)$$

$$d^9\ CLFSE(D_{4h}) = (-99e_\sigma + 72e_\pi)/45 \qquad (5)$$

$R = 15/8$, implying that e_π must be nearly twice the magnitude of e_σ to favour tetrahedral co-ordination. In fact *R* must be even larger since, for such big e_π values, there is an inversion of the T_d energy-level diagram which alters the CLFSE from $-(2/5)\Delta_{tet}$ to $-(3/5)\Delta_{tet}$. Equating equations (5) and (6) gives $R = 21/8$.

$$d^9\ CLFSE(T_d : e_\pi\ large) = (-36e_\sigma + 48e_\pi)/45 \qquad (6)$$

Thus, although it can be done, inducing tetrahedral co-ordination using the CLFSE alone leads to a change in ground state and unreasonably large values of e_π. Similarly, using the non-bonding repulsion term requires a 20-fold increase over the usual value of 49496 to favour a T_d geometry.

Table 5 Observed and calculated bond lengths (Å) and angles (°) for six-co-ordinate copper(II) complexes (see Fig. 1 for structural diagrams)

	$[Cu(amp)_3]^{2+}$		$[Cu(dpma)_2]^{2+}$		$[Cu(bipy)_3]^{2+}$	
	calc.	obs.[32]	calc.	obs.[33]	calc.	obs.[34]
$Cu-N_{am}$	1.93	2.05	1.99	2.02		
	2.01	2.01				
	2.09	2.04				
$Cu-N_{py}$	2.05	2.06	2.05	2.02	2.36	2.45
	2.45	2.44	2.51	2.54	2.36	2.23
	2.47	2.42			1.98	2.03
					1.96	2.03
					1.98	2.03
					2.00	2.03
N–Cu–N	173.0	166.4	71.2	72.2	79.7	78.2
	91.4	96	82.9	86.4	84.7	101.6
	95.4	89.5	108.8	107.8	99.0	99.5
	101.3	96.1	97.0	93.6	96.3	92.4
	82.5	73	80.9	79.8	92.0	91.6
	93.0	90.1	108.9	107.8	99.0	99.1
	91.2	103.9	99.1	100.2	96.2	94.4
	73.1	80.5	97.1	93.6	88.3	73.9
	93.5	94.3	99.1	100.2	88.1	94.1
	71.6	75.2	71.2	72.2	85.1	93.6
	172.2	163.8	82.9	86.4	91.9	92.2
	91.8	95.8	80.9	79.8	80.0	80.4
	94.1	94.2	180.0	180.0	178.4	174.8
	156.8	159.6	180.0	180.0	175.9	174.2
	104.0	98.1	180.0	180.0	176.3	165.6

	$[Cu(tpzm)_2]^{2+}$		$[Cu(Him)_6]^{2+}$		$[Cu(terpy)_2]^{2+}$	
	calc.	obs.[35]	calc.	obs.[36]	calc.	obs.[37]
$Cu-N_{pz}$	1.99	2.00	2.04	2.01		
	1.99	2.00	2.04	2.01		
	2.01	2.03	2.06	2.05		
	2.01	2.03	2.06	2.02		
	2.41	2.36	2.51	2.59		
	2.41	2.36	2.51	2.59		
$Cu-N_{py}$					1.83	1.98
					1.83	1.98
					2.27	2.18
					2.27	2.18
					2.27	2.18
					2.27	2.18
N–Cu–N	84.5	86.1	87.8	88.3	82.6	78.9
	79.5	81.5	92.1	92.1	85.0	87.8
	100.3	98.5	92.1	91.7	97.1	100.6
	95.4	93.9	87.9	87.9	97.5	96.0
	180.0	180.0	89.5	91.4	82.5	78.2
	85.5	86.8	92.1	92.1	97.3	96.8
	94.6	93.2	87.9	88.6	97.6	108.3
	180.0	180.0	90.5	91.4	97.2	97.0
	95.5	93.9	90.5	88.3	97.7	102.3
	180.0	180.0	87.9	88.6	84.1	89.2
	94.3	93.2	92.1	91.7	82.6	77.4
	100.3	95.5	89.5	87.9	82.6	77.5
	84.5	86.8	180.0	180.0	165.1	157.1
	79.7	81.5	180.0	180.0	165.1	154.9
	85.5	86.1	180.0	180.0	179.7	174.2

Of course, the experimental structure of $[CuCl_4]^{2-}$ has $\theta \approx 65$ rather than 90° but this still requires anomalously large increases in A and e_π. Conversely, if the non-bonding parameters are assigned their usual values (with $e_\pi = 0$ for the moment), a ligand charge of -0.7 gives $\theta = 67°$. We note that keeping everything else the same but increasing e_π to 2000 cm^{-1} gives $\theta = 65°$. Thus, π bonding does favour tetrahedral co-ordination but only to a relatively slight extent for any reasonable choice of e_π and the same effect can be achieved by reducing the magnitude of e_σ using a_0 of equation (3). Therefore, of the three methods for inducing a tetrahedral distortion, electrostatic interactions appear to be the most satisfying.

In the light of this analysis, charges were introduced into the force field for $[Cu(bipy)_2]^{2+}$. This necessitates changing the Cu–N Morse function parameters (see caption to Fig. 2) since, in a complete CLFSE/MM treatment, we require a counteracting positive charge on Cu in addition to ligand donor atom charges. This electrostatic interaction has a strong influence on the M–L stretching term. However, it is now possible to reproduce the experimental Cu–N distances to within 0.03 Å and the dihedral angle between the two bipy ligands to within 3°.

Table 6 Observed and calculated bond lengths (Å) and angles (°) for five- and four-co-ordinate copper(II) complexes (see Fig. 1 for structural diagrams)

	$[Cu(bipy)_2(NH_3)]^{2+}$		$[Cu(Him)_4]^{2+}$		$[Cu(aep)_2]^{2+}$		$[Cu(bipy)_2]^{2+}$	
	calc.	obs.[38]	calc.	obs.[39]	calc.	obs.[40]	calc.	obs.[41]
$Cu-N_{am}$	2.05	2.05			1.97	2.01		
$Cu-N_{py}$	1.96	2.05			2.00	2.02	2.19	1.97
	1.96	1.98					2.19	1.99
	1.99	2.11					1.82	1.99
	2.36	2.07					1.82	2.03
$Cu-N_{pz}$			2.03	2.01				
N–Cu–N	88.6	92.7	90.0	88.4	87.6	86.6	86.5	83.6
	179.5	129.5	90.0	88.4	87.6	86.6	94.5	102.3
	92.1	122.3	90.0	91.6	92.4	93.4	125.7	160.9
	92.8	91.5	90.0	91.6	92.4	93.4	177.7	151.1
	80.3	79.4	180.0	180.0	180.0	180.0	94.5	102.4
	90.8	98.0	180.0	180.0	180.0	180.0	86.5	81.3
	176.9	175.8						
	96.7	108.3						
	88.1	97.9						
	87.8	79.6						

N_{pz} is N in a five-membered ring, N_{py} is N in a six-membered ring.

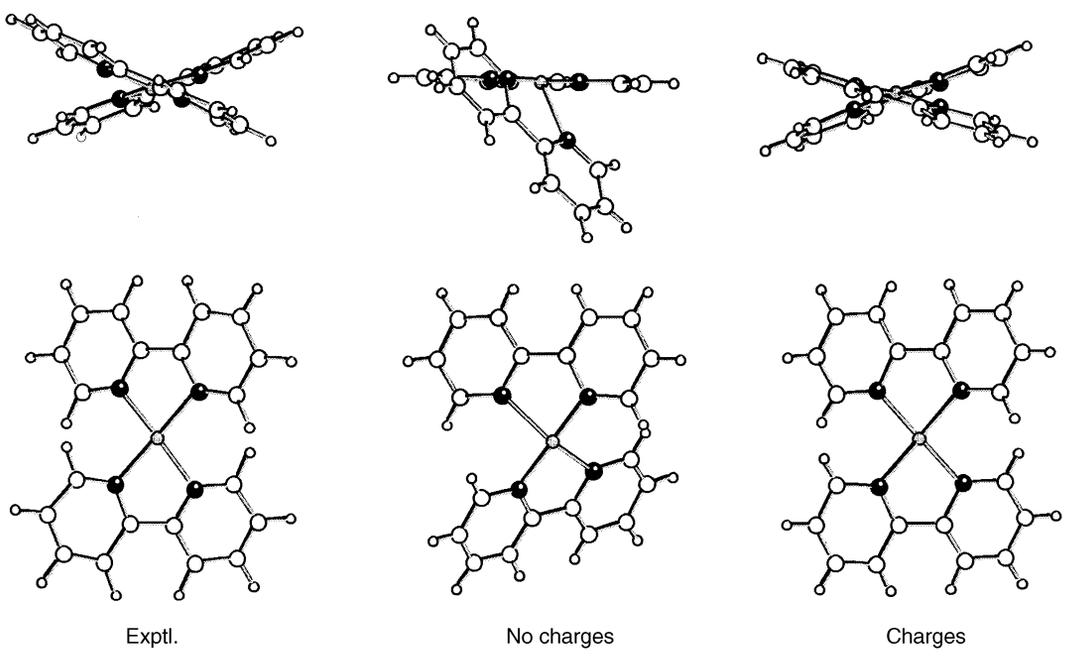

Fig. 2 Comparison of structures of $[Cu(bipy)_2]^{2+}$. Left, experiment;[38] centre, calculated structure without electrostatic interactions; right, calculated structure with electrostatic interactions. Force-field parameters for the latter are as given in SUP 57196 except for charges on Cu and N of +0.50 and −0.41 respectively and new Cu–N Morse function parameters of $D_0 = 120$ kcal mol^{-1}, $r_0 = 2.233$ Å and $\alpha = 0.45$

Conclusion

The CLFSE/MM method has successfully been extended to mixed-ligand complexes of Co^{III}, Ni^{II} and Cu^{II}. As a preliminary step, calculations on simple amine complexes of Co^{III} showed that the CLFSE/MM scheme can readily reproduce the performance of conventional MM methods. We then moved on to consider mixed amine–chloro complexes of Co^{III} and Ni^{II}.

Chloride ligands are potential π donors. However, an illustrative analysis of the CLFSE for octahedral complexes shows that for such ligands the increasingly positive value of e_π associated with a shorter, stronger M–L bond reduces Δ_{oct} and gives a less negative CLFSE. This arises because the d_π orbitals are lower than the (crystal field-like) barycentre. Thus, the π interaction works against σ bonding since the changes in the d_π energies *relative to the barycentre* are not a true reflection of the overall change in the electronic component of M–L π bonding. The CLFSE has the wrong form to produce the desired π contribution to the M–L bond length and we are obliged to remove any distance dependence and use a fixed value of e_π. This could still, in principle, influence the rotation about the M–L vector but not for d^8, d^9 and low-spin d^6 configurations since the d_π orbitals maintain their own barycentre and are symmetrically occupied for these configurations. Moreover, the effect of π bonding on L–M–L angle potentials is small, unless one entertains e_π values very much larger than those for e_σ, and can be accommodated by reducing the magnitude of the latter. In order to retain the very general description of the ligand-field potential in terms of spherical harmonics and the concomitant crystal field barycentre, we are forced to discard π contributions and retain the σ-only implementation of the CLFSE.

Fortunately, this method works remarkably well. The calcu-

lated structures for the eight chloro–amine MN_4Cl_2 complexes are in good agreement with experiment with the average r.m.s. error in M–L distances and L–M–L angles less than 0.03 Å and 3° respectively. The CLFSE term provides the 'through bond' communication between axial and equatotial ligands in the nickel(II) macrocyclic complexes such that the synergism observed experimentally is reproduced, *i.e.* as the equatorial Ni–N distances decrease the axial Ni–Cl bonds lengthen. The CLFSE/MM model is the first MM-based approach capable of treating this relatively subtle effect.

Calculations for imine and amine–imine $Ni^{II}N_6$ complexes also reproduce experiment well. In general, slightly poorer absolute agreement was found for comparable copper(II) systems but, given the plasticity of their co-ordination spheres, this result is not surprising. Jahn–Teller elongated structures are computed automatically for five of the six CuN_6 species and two of the three four-co-ordinate complexes have the required planar geometries. The three remaining systems, $[Cu(bipy)_2(NH_3)]^{2+}$, $[Cu(terpy)_2]^{2+}$ and $[Cu(bipy)_2]^{2+}$, appear at first sight to be treated less well but there are good reasons for this. First, for five-co-ordinate species, we have already noted[12] that while the CLFSE/MM scheme favours square-pyramidal co-ordination the trigonal-bipyramidal structure is very close in energy. Crystal-packing forces are sufficiently large that any structure between these two extremes may be observed. For $[Cu(bipy)_2(NH_3)]^{2+}$ the experimental structure happens to be near *TBPY* which emphasises the structural difference between the crystal and the computed structure. Energetically, however, the discrepancy between modelling and experiment is not significant. Similarly, the apparently incorrect compressed octahedral structure computed for $[Cu(terpy)_2]^{2+}$ is within 3 kcal mol^{-1} of the elongated structure. The nickel(II) analogue is also compressed. Evidently, the ligand is able to overcome the tetragonal elongation favoured by the CLFSE but for both $[Cu(terpy)_2]^{2+}$ and $[Cu(bipy)_2(NH_3)]^{2+}$ the energy differences between the minimised structure and those based on experiment are of the order of crystal-packing energies.

In contrast, $[Cu(bipy)_2]^{2+}$ is calculated to be too flat and crystal packing cannot be blamed. However, a simple treatment of D_{2d} $[CuCl_4]^{2-}$ shows that there are several mechanisms for forcing the geometry of four-co-ordinate copper(II) species away from the planar symmetry favoured by the CLFSE. One can make e_π significantly larger than e_σ or increase the non-bonding repulsion term four-fold or place a charge of −0.7 on the chloride ligands. The latter approach seems most reasonable and the explicit inclusion of 1,3 and 1,2 electrostatic interactions in a complete CLFSE/MM treatment gives the correct flattened tetrahedral structure for $[Cu(bipy)_2]^{2+}$. The ability to model charge effects is highly desirable anyway and we are presently developing a transferable force field which includes electrostatic interactions explicitly.

Appendix

CLFSE/MM modelling for D_{2d} MX_4 species with fixed M–X distance

The d-orbital energies can be expressed as a function of θ and the CLF parameters (note the *x* and *y* axes have been rotated through 45° relative to the conventional D_{2d} definition), equations (A1)–(A4). The energy barycentre, E(BC), is given by

$$E(d_{z^2}) = 4e_\sigma[\tfrac{1}{4}(1 + 3\cos 2\theta)]^2 + 4e_\pi(\sqrt{\tfrac{3}{2}}\sin 2\theta)^2 \quad (A1)$$

$$E(d_{xz}, d_{yz}) = 2e_\sigma(\sqrt{\tfrac{3}{2}}\sin 2\theta)^2 + 2e_\pi(\cos^2 2\theta + \cos^2\theta) \quad (A2)$$

$$E(d_{x^2-y^2}) = 4e_\sigma[\sqrt{\tfrac{3}{4}}(1 - \cos 2\theta)]^2 + e_\pi \sin^2 2\theta \quad (A3)$$

$$E(d_{xy}) = 4e_\pi \sin^2\theta \quad (A4)$$

equation (A5). Thus, given that $d_{x^2-y^2}$ is the highest-energy d

$$E(\mathrm{BC}) = \tfrac{1}{5}(4e_\sigma + 8e_\pi) \quad (A5)$$

orbital, the CLFSE is given by equation (A6). The D_{2d} symmetry ensures there are no off-diagonal elements in the ligand-field potential matrix so the CLFSE can be computed directly based on equations (A1)–(A5). Also, equation (A6) is easily modified to account for changes in the nature of the singly occupied d orbital such as occur when e_π is very much larger than e_σ.

$$\mathrm{CLFSE} = 2E(d_{xy}) + 4E(d_{xz}, d_{yz}) + 2E(d_{z^2}) + E(d_{x^2-y^2}) - 9E(\mathrm{BC}) \quad (A6)$$

The non-bonding term E_{vdw} has the form (A7) where r represents the interatomic distance. For a fixed M–X bond length, r_0, only the six unique X ··· X distances need to be considered, two long contacts of length $2r_0\sin\theta$ and four short contacts of length $[2r_0^2(1 + \cos^2\theta)]^{\frac{1}{2}}$. The total non-bonding interaction is thus a simple sum over these six distances.

$$E_{vdw} = (A/r^6) - (B/r^9) \quad (A7)$$

The same arguments apply to computing the electrostatic interaction. Each component, E_C, is given by equation (A8) and the total electrostatic energy is a sum over the six unique X ··· X distances.

$$E_C = q^2/r \quad (A8)$$

Finally, the total energy, E_{tot}, is the sum of these three interactions after due care is taken to ensure that each energy term is expressed in the same units, equation (A9).

$$E_{tot}(D_{2d}) = \mathrm{CLFSE} + \Sigma E_{vdw} + \Sigma E_c \quad (A9)$$

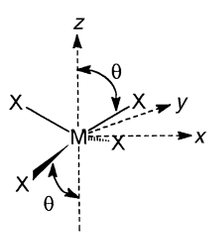

Acknowledgements

The authors acknowledge the financial support of the Vice Chancellor's Infrastructure Fund and the EPSRC for the provision of a studentship (to V. J. P.).

References

1 V. J. Burton, R. J. Deeth, C. M. Kemp and P. J. Gilbert, *J. Am. Chem. Soc.*, 1995, **117**, 8407.
2 P. Comba and T. W. Hambley, *Molecular Modelling of Inorganic Compounds*, VCH, Weinheim, 1995.
3 P. V. Bernhardt and P. Comba, *Inorg. Chem.*, 1992, **33**, 2638.
4 P. V. Bernhardt, P. Comba, T. W. Hambley, S. S. Massoud and S. Stebler, *Inorg. Chem.*, 1992, **31**, 2644.
5 R. K. Adam, M. Antolovich, L. G. Brigden and L. F. Lindoy, *J. Am. Chem. Soc.*, 1991, **113**, 3346.
6 B. P. Hay, *Coord. Chem. Rev.*, 1993, **126**, 177.
7 P. Comba, T. W. Hambley and L. Zipper, *Helv. Chim. Acta*, 1988, **71**, 1875.
8 T. W. Hambley, *Inorg. Chem.*, 1988, **27**, 1073.
9 T. W. Hambley, *J. Chem. Soc., Dalton Trans.*, 1986, 565.

10 T. W. Hambley, C. J. Hawkins, J. A. Palmer and M. R. Snow, *Aust. J. Chem.*, 1991, **34**, 45.
11 R. D. Hancock, S. M. Dobson, A. Evers, P. W. Wade, M. P. Ngwenya and J. C. A. Boeyens, *J. Am. Chem. Soc.*, 1988, **110**, 2788.
12 V. J. Burton and R. J. Deeth, *J. Chem. Soc., Chem. Commun.*, 1995, 573.
13 M. Gerloch, *Magnetism and Ligand Field Analysis*, Cambridge University Press, New York, 1983.
14 M. Gerloch, J. H. Harding and R. G. Woolley, *Struct. Bonding* (*Berlin*), 1981, **46**, 1.
15 Cambridge Structural Database, Version 4, Cambridge Crystallographic Data Centre, University Chemical Laboratory, Cambridge, 1994.
16 E. O. Schlemper, *J. Cryst. Mol. Struct.*, 1977, **7**, 81.
17 E. N. Duesler and K. N. Raymond, *Inorg. Chem*, 1971, **10**, 1486.
18 R. Nagao, F. Marumo and Y. Saito, *Acta Crystallogr., Sect. B*, 1973, **29**, 2438.
19 T. W. Hambley, G. H. Searle and M. R. Snow, *Aust. J. Chem.*, 1982, **35**, 1285.
20 K. Matsumoto, S. Ooi and H. Kuroya, *Bull. Chem. Soc. Jpn.*, 1970, **43**, 3801.
21 A. S. Foust and V. Janickis, *Inorg. Chem.*, 1980, **19**, 1048.
22 J. D. Mather, R. E. Tapscott and C. F. Campana, *Inorg. Chim. Acta*, 1983, **73**, 235.
23 T. Ito and K. Toriumi, *Acta Crystallogr., Sect. B*, 1981, **37**, 88.
24 T. Ito, M. Kato and H. Ito, *Bull. Chem. Soc. Jpn.*, 1984, **57**, 2641.
25 M. Sugimoto, J. Fugita, H. Ito, K. Toriumi and T. Ito, *Inorg. Chem.*, 1983, **22**, 955.
26 A. A. Watson, D. A. House and P. J. Steel, *Inorg. Chim. Acta*, 1987, **130**, 167.
27 J. P. Konopelski, C. W. Reimann, C. R. Hubbard, A. D. Mighell and A. Santoro, *Acta Crystallogr., Sect. B*, 1976, **32**, 2911.
28 A. Wada, N. Sakabe and J. Tanaka, *Acta Crystallogr., Sect. B.*, 1976, **32**, 1121.
29 M. I. Arriortua, T. Rojo, J. M. Amigo, G. Germain and J. P. Declercq, *Bull. Soc. Chim. Belg.*, 1982, **91**, 337.
30 P. V. Bernhardt, P. Comba, A. Mahu-Rickenbach, S. Stebler, S. Steiner, K. Varnagy and M. Zehnder, *Inorg. Chem.*, 1992, **31**, 4194.
31 C. W. Reinann, A. Santoro and A. D. Mighell, *Acta Crystallogr., Sect. B*, 1970, **26**, 521.
32 A. W. Maverick, M. L. Ivie and F. R. Fronczek, *J. Coord. Chem.*, 1990, **21**, 315.
33 P. V. Bernhardt, P. Comba, A. Mahu-Rickenbach, S. Stebler, S. Steiner, K. Varnagy and M. Zehnder, *Inorg. Chem.*, 1992, **31**, 4194.
34 O. P. Anderson, *J. Chem. Soc., Dalton Trans.*, 1972, 2597.
35 T. Astley, J. M. Gulbis, M. A. Hitchman and E. R. T. Tiekink, *J. Chem. Soc., Dalton Trans.*, 1993, 509.
36 D. L. McFadden, A. T. McPhail, C. D. Garner and F. E. Mabbs, *J. Chem. Soc., Dalton Trans.*, 1975, 263.
37 J. V. Folgado, W. Henke, R. Allmann, H. Stratmeier, D. Beltran-Porter, T. Rojo and D. Reinen, *Inorg. Chem.*, 1990, **29**, 2035.
38 F. S. Stephens, *J. Chem. Soc., Dalton Trans.*, 1972, 1350.
39 G. Fransson and B. K. S. Lundberg, *Acta Chem. Scand.*, 1972, **26**, 3969.
40 D. L. Lewis and D. J. Hodgson, *Inorg. Chem.*, 1974, **13**, 143.
41 H. Nakai, *Bull. Chem. Soc. Jpn.*, 1971, **44**, 2412.
42 R. D. Hancock, *Prog. Inorg. Chem.*, 1989, **37**, 187.
43 T. Ito, M. Kato and H. Ito, *Bull. Chem. Soc. Jpn.*, 1984, **57**, 1556.
44 P. B. Hitchcock, K. R. Seddon and T. Welton, *J. Chem. Soc., Dalton Trans.*, 1993, 2639.
45 R. Allmann, W. Henke and D. Reinen, *Inorg. Chem.*, 1978, **17**, 378.
46 R. J. Deeth and M. A. Hitchman, *Inorg. Chem.*, 1986, **25**, 1225.
47 W. D. Harrison, D. M. Kennedy, M. Power, R. Sheahen and B. J. Hathaway, *J. Chem. Soc.*, 1963, 1556.
48 G. A. Barely, B. F. Hoskins and C. H. C. Kennard, *J. Chem. Soc.*, 1963, 5691.
49 K. E. Halvarson, C. Patterson and R. D. Willett, *Acta Crystallogr., Sect. B*, 1990, **46**, 508.
50 P. D. Sheen, Ph.D. Thesis, 1995, Bath University; K. Waizumi, H. Masuda, H. Einaga and N. Fukushima, *Chem. Lett.*, 1993, 1145.

Received 16*th September* 1996*; Paper* 6/06381K